Optical investigation of CdTe monomolecular islands in wide ZnTe/(Zn,Mg)Te quantum wells: Evidence of a vertical self-ordering

Pierre Lefebvre and Vincent Calvo
Groupe d'Etude des Semiconducteurs, CNRS, Université Montpellier II, Case courrier 074, 34095 Montpellier Cedex 5, France

Noël Magnea
C.E.A. Grenoble, Département de Recherche Fondamentale sur la Matière Condensée/SP2M. 17, avenue des Martyrs, 38054 Grenoble, France

Thierry Taliercio, Jacques Allègre, and Henry Mathieu
Groupe d'Etude des Semiconducteurs, CNRS, Université Montpellier II, Case courrier 074, 34095 Montpellier Cedex 5, France
(Received 24 March 1997)

Continuous, piezomodulated, and time-resolved optical spectroscopies have been carried out on several samples basically consisting of a 38-nm-wide ZnTe quantum well incorporating monomolecular CdTe islands grown by molecular-beam epitaxy on nominal (001) ZnTe surfaces. During the growth of some samples, five regularly spaced monomolecular layers (single or half-monolayers) of CdTe were inserted in the wide ZnTe quantum wells. Our results indicate that, under certain conditions of deposition, (i) the fractional layers constitute CdTe islands separated by ZnTe ''voids,'' with in-plane size and spacing quite larger than the exciton Bohr diameter; and (ii) when several fractional monolayers are grown, these islands tend to stack on top of each other. The effects of this vertical self-ordering disappear when the conditions of deposition are changed. Moreover, it is shown that the CdTe inserts act as giant isoelectronic recombination centers, yielding intense and sharp photoluminescence lines with very short decay times (a few tens of picoseconds) in the range of $\lambda \approx 517$ nm. [S0163-1829(97)01831-6]

I. INTRODUCTION

Much attention has been paid recently to the possibility of self-organized crystal epitaxy of nanometric objects such as semiconductor quantum dots. Basically, such ordered growth is induced by the strong difference of lattice parameters between the epitaxial layer and the substrate. In some instances, the resulting strain is capable of producing a nanoscaled surface morphology, which is the origin of the growth of small islands. Most breakthroughs in this field have been obtained with III-V semiconductors.[1–5] A significant enhancement of quantum yield has been observed in such samples, although systematically disturbed by inhomogeneous broadening due to size-distributed dots. Moreover, it has been shown[2] that a vertical ordering of the islands occurs when several layers of such islands are grown, separated by a few planes of the host material.

Recent investigations[6–9] have provided a strong indication of the presence of comparable vertically ordered growth of ZnTe monomolecular islands in CdTe-(Cd,Zn)Te quantum well systems. In this particular case, ZnTe half-monolayers, deposited during the growth of a CdTe quantum well, tend to constitute pavements of rather wide ZnTe islands. It has been found that the islands of two fractional layers, separated by a few CdTe layers, adopt a staggered vertical lineup, as a result of strong in-plane and on-axis deformations. This particular lineup was tentatively related[9] to the relative stiffnesses of the host material (CdTe) and of the inserts (ZnTe), by reference to existing theories developed for metallic precipitates.[10,11] If the material of the islands is softer than that of the matrix, an interplane attraction causes the islands to grow ''on top of each other:'' this is the case of InAs quantum dots embedded in GaAs. Conversely, ZnTe is harder than CdTe; then, ZnTe islands tend to repel each other and to adopt a vertical staggered lineup.

Consequently, it is expected that comparable inserts of CdTe in a ZnTe environment should now grow in the opposite way, i.e., with CdTe islands vertically stacked on top of each other, just like InAs in GaAs. In addition, contrary to ZnTe islands, which act as potential barriers for electrons and heavy holes, CdTe inserts should play the role of isoelectronic recombination centers for excitons, since they constitute potential wells for electrons, light holes, and heavy holes.

In this paper, we demonstrate from optical spectroscopy that, under certain conditions, vertically ordered CdTe islands, separated by ZnTe spacers, can be grown on nominal (001) ZnTe substrates. In the present case, the in-plane average size and spacing of the islands are likely to be large compared to the exciton Bohr diameter ($d_B \sim 10$ nm). Moreover, we show that such an in-plane superstructure can be modified or suppressed by changing growth conditions, and that the presence of CdTe inserts yields intense and sharp photoluminescence lines with very short decay times (under 100 ps) around $\lambda = 520$ nm.

II. EXPERIMENTAL DETAILS

A. Sample growth

All samples grown by molecular-beam epitaxy (MBE) basically consist of a wide ZnTe quantum well with potential

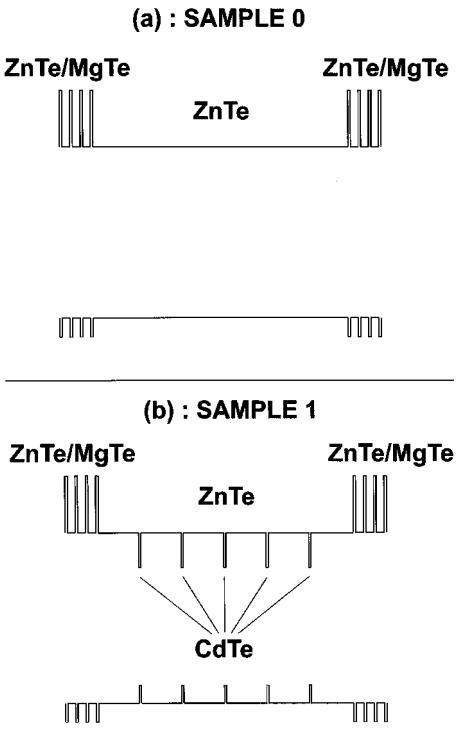

FIG. 1. Sketch of the typical band profiles for electrons and heavy holes, along the z axis in our samples, as deduced from band offsets and strain effects usually encountered in CdTe-(Cd/Zn)Te systems. All growths were made on the (001) surface of a ZnTe substrate. (a) The case of sample 0, where barriers made of ZnTe-MgTe short-period superlattices surround a 120-ML ZnTe quantum well. (b) The case of sample 1, in which single monolayers of CdTe have been grown, separated by 20 ML of ZnTe.

barriers made of short-period ZnTe-(Zn,Mg)Te superlattices, grown on nominal (001) surface of ZnTe substrates. Sample 0, of which a band profile in the z direction is sketched in Fig. 1(a), is constituted just by this reference structure, i.e., the ''bare'' 120 ML wide (36 nm) ZnTe quantum well. In fact, the barrier superlattice in sample 0 has a slightly smaller effective gap than those in samples 1–3, due to a different composition of the barrier superlattice, essentially.

Concerning the other samples, during the growth of the ZnTe well, every 20 ML, an integer or half-monolayer of CdTe has been deposited, yielding the typical band profile shown in Fig. 1(b), which is the case of sample 1, with five full ML's. Samples 2 and 3 both contain half-monolayers of CdTe: the five corresponding planes nominally contain an equal quantity of Cd and Zn atoms. CdTe and ZnTe growth rates are deduced from reflection high-energy electron-diffraction oscillations with an accuracy of $\pm 5\%$.

Now, the fractional layers in sample 2 have been obtained by the usual MBE, i.e., by growing CdTe in a classical way, but just for the time required for filling half a plane, then completed with ZnTe. This permits the formation of CdTe islands, separated by ZnTe areas. On the other hand, for sample 3, the CdTe half-plane was grown by the so-called atomic layer epitaxy (ALE) method.[12] Cd and Te cells were opened one at a time. This induces a self-regulation process, which allows the control of the growth with a half-atomic plane accuracy. In the present case, the Cd atoms deposited are almost homogeneously distributed in their respective planes, occupying one anion site over two. The present half-monolayers are then likely to behave like monolayers of a quasiperiodic $Cd_{0.5}Zn_{0.5}Te$ alloy.

B. Optical spectroscopy

Continuous reflectivity and photoluminescence (PL) experiments were conducted with the same conventional setup: the samples were immersed in a pumped liquid-helium bath cryostat ($T \sim 2$ K) and illuminated either by an Ar^{++} laser (PL experiments) or by a 100-W tungsten wire lamp (reflectivity). The emitted or reflected signals were dispersed through a HRS Jobin-Yvon spectrometer, and detected by a photomultiplier in the standard synchronous mode.

For piezomodulation experiments, a cold-finger cryostat with liquid-He circulation, giving a sample temperature of ~ 10 K, was used; the samples were glued onto a piezoelectric transducer, driven by an alternating voltage, so as to undergo a small, alternating in-plane biaxial strain. The differential spectra were then obtained by detecting the signal variations synchronously with the driving voltage. This is known to provide a signal proportional to the first-order derivative of the direct signal, but with coefficients depending on the symmetry of the valence-band states (light or heavy holes) involved in the optical transition.[9,13–15] This selective modulation thus gives a straightforward identification of the observed spectral features in terms of light- or heavy-hole excitons.

Time-resolved PL experiments have been conducted by using the following setup: The samples were kept at a minimum temperature of ~ 8 K on the cold finger of a helium closed-cycle cryostat. They were excited by ~ 2-ps laser pulses, centered at $\lambda \sim 400$ nm, with a repetition frequency of 82 MHz. These pulses were obtained from the $\lambda \sim 800$ nm pulses of a Ti-sapphire cavity, by using a lithium triborate frequency doubler. The emitted light was dispersed through a 500SM Chromex spectrometer, with a 500-mm focal length and a 1200-g/mm grating, and detected by a Hamamatsu C4334 streakscope. The temporal response of this setup to ultrashort laser excitation is broadened to a typical full width at half maximum of ~ 15 ps. Thus the temporal resolution of the setup, after deconvolution of the PL decay from this response, is of the order of 5 ps.

III. EXPERIMENTAL RESULTS

Figures 2–5 display the PL and reflectance spectra of samples 0–3, respectively, obtained at $T = 2$ K. PL spectra have been plotted on a logarithmic scale, so as to emphasize weaker contributions, but the full widths at half maximum of the fundamental transitions are mentioned in the figures. Common to all spectra are the reflectance features around 2.383 eV, assigned to the free exciton (FE) in the substrates of bulk ZnTe. To this transition correspond, in all samples, the weak high-energy feature of the PL of the substrate. At slightly lower energy (~ 2.375 and 2.378 eV), lie PL lines assigned to bound excitons (BE's) in the substrates. Now, common to samples 1–3, but at varying energies, are the features denoted $e1h1$ and $e1l1$, characteristic of excitons confined in the CdTe inserts. These notations are inspired with those commonly used for wider CdTe quantum wells. The $e1h1$ and $e1l1$ transitions are also observed in PL spec-

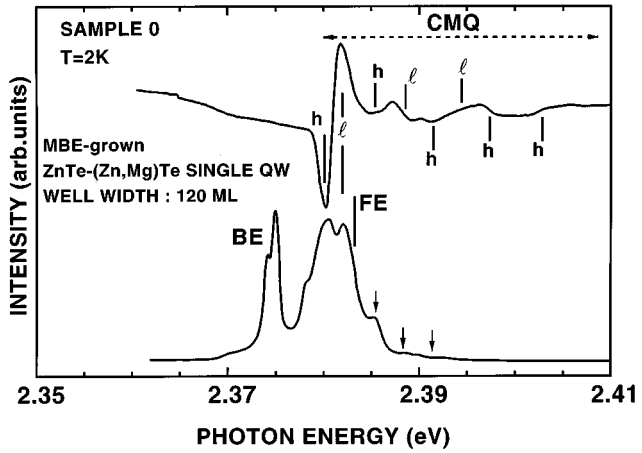

FIG. 2. Photoluminescence (PL) and reflectance spectra of sample 0, taken at $T=2$ K. FE denotes the degenerate heavy- and light-hole free exciton of the substrate. BE stands for bound excitons in the substrate. CMQ represents the series of reflectance and PL features assigned to the quantization of motion of the center-of-mass of excitons in the 120-ML-wide ZnTe quantum well.

tra, with no redshift relatively to reflectance features (except a very small one for sample 1, probably due to excitons trapped on layer thickness fluctuations). Going from sample 1 to sample 3, both transitions shift towards high energy, while their full widths at half maximum decrease.

The light- or heavy-hole characters have been clearly assigned by using selective piezoreflectance measurements. Due to the values of deformation potentials in the present ZnTe-rich structures, reflectivity features related to light-hole excitons are ''piezoderivated'' ~2.3 times more than those related to heavy-hole excitons. This technique allows us to confirm the characters of transitions $e1h1$ and $e1l1$, and of the split heavy- and light-hole excitons in the barrier superlattices (not shown here). Careful inspection of the spectra also allows us to identify light- and heavy-hole characters among all the reflectance features above the band gap of ZnTe, observed in samples 0 and 2, as marked by ''l'' and ''h'' in Figs. 2 and 4. For the other samples, this was quite uneasy due to the weakness of similar reflectance structures and to their intricate overlapping.

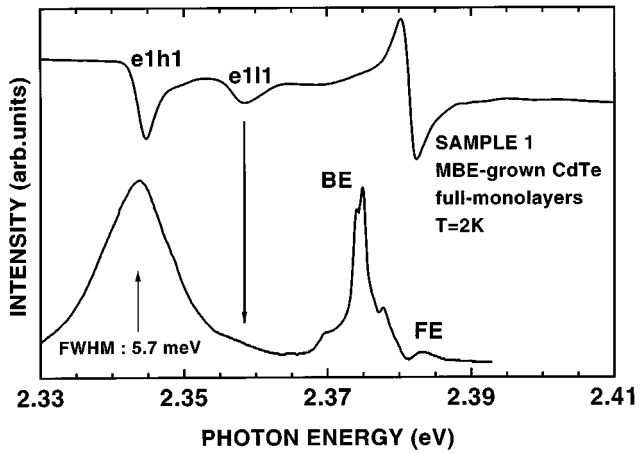

FIG. 3. The same as Fig. 2, for sample 1. $e1h1$ and $e1l1$ represent the heavy- and light-hole excitons trapped on CdTe inserts.

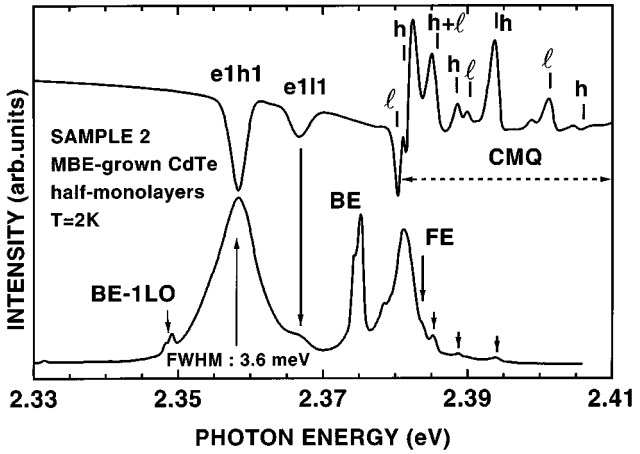

FIG. 4. Reflectance and PL spectra of sample 2. The sharp features associated with the CMQ regime have been identified in terms of light- or heavy-hole excitons, as shown by ''l'' or ''h.'' The free exciton of the substrate (FE) has a mixed ($l+h$) character.

Although these high-energy transitions are observed by reflectivity in all samples, they are strong only for samples 0 and 2. Moreover, these transitions appear *in both reflectance and PL spectra* only in these two samples: in PL spectra, several excited transitions corresponding to reflectance structures are observed, with a prominent contribution of heavy-hole excitons. We assign these transitions to the states of excitons confined in the wide ZnTe well, in the so-called ''center-of-mass motion quantization'' (CMQ) regime. This observation has already been made in wide CdTe/(Cd,Zn)Te quantum wells, but for the only heavy-hole excitons[16] because lattice-mismatch strains put the light-hole excitons into a type-II band lineup in these materials. Quite similarly, such CMQ states for both heavy- *and* light-hole excitons are observed in the present samples. A detailed study of this observation in terms of confined excitonic-polariton modes will be published elsewhere.[17] The appearance of these states is favored by the large well width (~38 nm), compared to the exciton Bohr diameter in ZnTe (~10 nm). The existence of

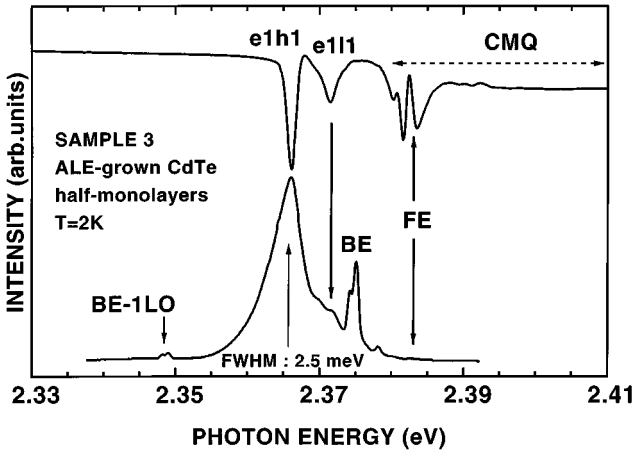

FIG. 5. Reflectance and PL spectra of sample 3. Note that reflectance features related to ''CMQ-like'' states are observed below and above the FE transition, but no PL line corresponds to these features. The small PL peak at 2.373 eV is characteristic of the substrate.

light- and heavy-hole exciton-polariton states is well known in zinc-blende semiconductors, like GaAs (Ref. 18) or ZnSe,[19] and models exist for the description of the corresponding threefold dispersion relation.[20] In brief, the dispersion curve of the ''excitonlike'' branch, at large k, is split into two contributions. For k sufficiently larger than the effective wave vector of light near the resonance, these contributions correspond respectively to the dispersion curves of particles having the following total masses $M_h = m_e + (\gamma_1 - 2\gamma_2)^{-1}$ and $M_l = m_e + (\gamma_1 + 2\gamma_2)^{-1}$. Although rigorous approaches[21] have been developed to account for optical spectra in case of CMQ, a simple model provides a satisfactory description of the present experimental data. For sample 2, the experimental light- and heavy-hole exciton energies have been fitted by theoretical quantization energies of particles of masses M_h and M_l in an infinitely deep quantum well, versus the quantum number N. Of course, the ''effective well width'' has been taken as a fitting parameter, since the potential wells for light- and heavy-hole excitons are finite (and different). Moreover, this width may be smaller than the physical width of the well (38 nm), due to the so-called ''dead layer'' near the well boundaries where the center-of-mass of the exciton cannot exist as such. However, in case of small confinement potential, as for samples 0 and 2, the exciton center of mass may be able to penetrate into the barrier superlattices.

For sample 2, the energy difference for excitons between ZnTe and the barrier superlattice has been measured as ~80 meV for heavy holes and ~110 meV for light holes. A problem arises from the fact that the lowest CMQ mode in sample 2 is ''light-hole-like,'' which we attribute to a small residual biaxial tension of the ZnTe layer, which may origin from the presence of MgTe and CdTe. Accounting for this strain, the effective widths obtained by the present fitting, for sample 2, are 24 and 26 nm for the light- and heavy-hole excitons, i.e., dead layers of 7 and 6 nm, respectively. This result is consistent with the fact that the potential barrier is higher for light-hole excitons than for heavy-hole excitons. It is also consistent with the fact that the reduced mass of electron-hole pairs is anisotropic, due to the lifting of degeneracy of valence bands. This causes, in particular, the on-axis effective Bohr radius to be larger for light-hole excitons than for heavy-hole ones, while the opposite is true in the plane of the layers. Then the center-of-mass of the heavy-hole exciton can come closer to the well-barrier interface than that of the light-hole exciton.

The differences in the spectra of samples 2 and 0 are mainly due to the difference in their barrier superlattices. For sample 0, we measured excitonic gap differences of 50 meV for heavy holes and 60 meV for light holes, between well and barriers. The fitting procedure then yields effective well widths of 39 and 40 nm, respectively, for light- and heavy-hole excitons. Such large values are consistent with the small confinement potentials.

Anyway, the above values are only indicative, considering the simplicity of the model. Moreover, a correct fitting procedure should include the strong nonparabolicity of dispersion curves which arises from exciton-photon coupling (the polariton effect), which is responsible, to our opinion, for the observation of the first CMQ resonances *below* the excitonic gap of bulk ZnTe. This point will be developed in a forthcoming paper.[17]

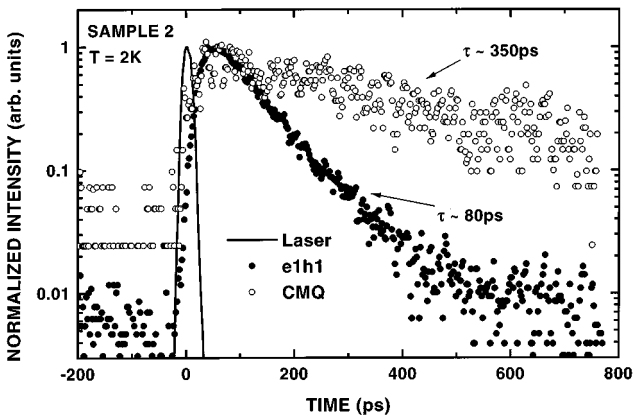

FIG. 6. Time decays of the normalized PL intensities, in sample 2, of transition $e1h1$ (solid circles) and of the recombination of the first exciton state of the 38-nm-wide ZnTe/(Zn,Mg)Te quantum well, confined in the so-called center-of-mass motion quantization (CMQ) regime (open circles). The excitation wavelength is 400 nm.

Now it is crucial to note that PL features related to the CMQ are only seen in samples 2 and 0, and that the corresponding reflectance features are stronger in these samples. Indeed, samples 1 and 3 also show relatively weak reflectance structures above 2.383 eV, assigned to excited states, above the edge of the CdTe quantum wells. These states are basically comparable to those produced by the CMQ, but efficient thermalization processes from them to the states of the CdTe traps prevent their observation by low-temperature PL. Obviously, this thermalization is impossible in sample 0, because the traps do not exist: then, a sequence of CMQ-related exciton states are observed in PL, similar to what has been observed in wide CdTe quantum wells. Now, the fact that such PL lines are also seen in sample 2 indicates that, either this thermalization and/or trapping is inefficient, or that the CdTe traps are saturated. Now, decreasing excitation intensity produces no particular change in the overall PL spectrum. Moreover, the results of time-resolved PL experiments on sample 2 are shown in Fig. 6. They reveal that the $e1h1$ line has an exponential decay time of ~80 ps, while the ground CMQ exciton line rather vanishes on a ~350-ps scale. If both recombination channels were connected, e.g., by an efficient trapping mechanism, the excited transition should show the same short-time decay as the fundamental one.

The above results thus prove that, in sample 2, excitons typical of an ''empty'' 38-nm-wide ZnTe quantum well can exist and recombine radiatively with their own decay rate (~350 ps) without being trapped into CdTe islands. Simultaneously, excitons trapped on these inserts recombine independently—and more rapidly. These remarks imply two important points: First, the in-plane dimension of CdTe islands and of interisland spacing in sample 2 are large enough, compared to the exciton Bohr diameter, to prevent the systematic trapping of excitons. Second, there must be ''clearings'' in the sample where the motion of excitons along the growth axis can take place from one side of the wide ZnTe well to the other, without meeting any cadmium atom. Consistently, in samples 1 and 3, where cadmium at-

oms are likely to be homogeneously distributed in their layer planes, the excitons cannot avoid falling into CdTe traps. This explains that CMQ-like exciton states are not observed in PL, even when increasing the excitation intensity. In particular, in sample 3, it is most probable that the ALE growth yields extremely efficient traps, as shown by the narrow and intense PL line of the $e1h1$ exciton. This shows one of the major interests of the ALE growth of submonolayers, which is to prevent ''faults'' or layer thickness fluctuations like those which probably occur in sample 1, as shown by the broader PL and reflectance features of the $e1h1$ exciton.

Concerning the observed blueshift of the $e1h1$ and $e1l1$ features when going from sample 1 to sample 3, it is difficult to invoke crudely lateral confinement effect, at least in the usual sense of the constitution of ''flat'' quantum dots. Envelope-function calculations are irrelevant in the present case. A model yielding the electronic structure of planes (or fractions of planes) of strongly relaxed cadmium atoms in substitutional position in the ZnTe lattice would be useful to explain the present blueshift. Moreover, if such a lateral confinement was present, it should be accompanied by usual size-distribution effects, i.e., the broadening of spectral features, which is not the case.

IV. CONCLUSION

Our interpretation of the present experimental findings is summarized by the sketch in Fig. 7. Sample 1 constitutes a kind of superlattice, where excitons are weakly bound to CdTe layers. States of the wide ZnTe well are defined here as ''resonant'' states above the edge of the CdTe wells. This explains the weak reflectance structures above 2.383 eV. However, these excited states do not contribute to PL recombinations. On the other hand, the observation of sharp reflectance structures *and* of PL features characteristic of the CMQ, in sample 2, can only be explained by (i) the presence of rather wide islands separated by wide spacings, and (ii) the vertical stacking of CdTe inserts. Consistently, if the cadmium atoms are homogeneously distributed in their planes (sample 3) we have a kind of shallow $Cd_{0.5}Zn_{0.5}Te/ZnTe$ superlattice, yielding a somewhat delocalized ground state for excitons. The excitons cannot avoid falling onto this state before recombination, although the CMQ states of the wide ZnTe well are defined.

We have thus obtained a clear indication that CdTe islands embedded in a ZnTe matrix can be grown with a vertical correlation. This ordering is comparable to that of InAs islands in GaAs. Moreover, recent theoretical investigations[22,23] suggest that this vertical correlation may result in a horizontal ordering of the islands, if a sufficient number of layers are grown. Thus here we have a promising route toward the preparation of three-dimensional arrays of islands, which act as isoelectronic traps for excitons. It is now expected that, by varying the growth conditions, one could produce CdTe quantum dots with variable lateral and vertical sizes and with variable lateral and vertical spacing. Deeper isoelectronic traps could then be obtained for excitons, which would operate strong confinement effects, such as the enhancement of the exciton binding energy and oscillator strength. In addition, the present results already show the large efficiency of the green PL in our ZnTe-based samples, comparable to the enhancement observed in III-V submonolayer systems.[3,4] Preliminary attempts show, in particular that this green PL remains strong at $T \sim 100$ K; systematic studies of the temperature behavior are under way.

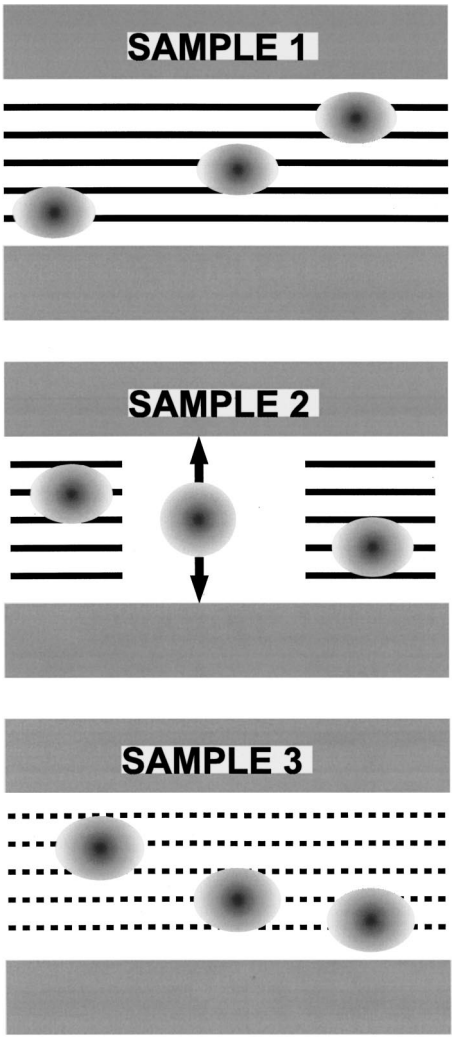

FIG. 7. A sketch of the real-space configurations of monomolecular CdTe insets in samples 1–3, as inferred from our optical data. Gray areas represent ZnTe-MgTe barrier superlattices, and bold lines show the positions of the insets. The oval and circular figures just indicate the typical shapes and dimensions of excitons in the structure.

[1] J. Y. Marzin, J. M. Gérard, A. Izrael, D. Barnier, and G. Bastard, Phys. Rev. Lett. **73**, 716 (1994).
[2] Q. Xie, A. Madhukar, P. Chen, and N. P. Kobayashi, Phys. Rev. Lett. **75**, 2542 (1995).
[3] P. D. Wang, N. N. Ledentsov, C. M. Sottomayor Torres, P. S. Kop'ev, and V. M. Ustinov, Appl. Phys. Lett. **64**, 1527 (1994).
[4] W. Li, Z. Wang, J. Liang, B. Xu, Z. Zhu, Z. Yuan, and J. Li, Appl. Phys. Lett. **67**, 1874 (1995).
[5] P. Castrillo, D. Hessman, M.-E. Pistol, S. Anand, N. Carlsson, W. Seifert, and L. Samuelson, Appl. Phys. Lett. **67**, 1905 (1995); D.

Hessman, P. Castrillo, M.-E. Pistol, C. Pryor, and L. Samuelson, *ibid*. **69**, 749 (1996).
[6] N. Magnea, J. Cryst. Growth **138**, 550 (1994).
[7] Q. X. Zhao, N. Magnea, and J. L. Pautrat, Phys. Rev. B **52**, 14 688 (1995).
[8] Q. X. Zhao, N. Magnea, and J. L. Pautrat, J. Cryst. Growth **159**, 425 (1996).
[9] V. Calvo, P. Lefebvre, J. Allègre, A. Bellabchara, H. Mathieu, Q. X. Zhao, and N. Magnea, Phys. Rev. B **53**, R16 164 (1996).
[10] A. J. Ardell, B. R. Nicholson, and J. D. Eshelby, Acta Metall. **14**, 1295 (1966).
[11] W. C. Johnson, Acta Metall. **32**, 465 (1983).
[12] J. M. Hartmann, G. Feuillet, and M. Charleux, J. Appl. Phys. **79**, 3035 (1996).
[13] H. Mathieu, P. Lefebvre, J. Allègre, B. Gil, and A. Regreny, Phys. Rev. B **36**, 6581 (1987).
[14] H. Mathieu, J. Allègre, and B. Gil, Phys. Rev. B **43**, 2218 (1991).
[15] J. Calatayud, J. Allègre, P. Lefebvre, and H. Mathieu, Mater. Sci. Eng. **16**, 87 (1993).
[16] H. Tuffigo, R. T. Cox, N. Magnea, Y. Merle d'Aubigné, and A. Million, Phys. Rev. B **37**, 4310 (1988).
[17] P. Lefebvre, V. Calvo, N. Magnea, T. Taliercio, J. Allègre, and H. Mathieu (unpublished).
[18] R. G. Ulbrich and C. Weisbuch, Phys. Rev. Lett. **38**, 865 (1977).
[19] B. Sermage and G. Fishman, Phys. Rev. Lett. **43**, 1043 (1979); Phys. Rev. B **23**, 5107 (1981).
[20] G. Fishman, Solid State Commun. **27**, 1097 (1978).
[21] A. D'Andrea and R. Del Sole, Europhys. Lett. **11**, 169 (1990); Phys. Rev. B **41**, 1413 (1990).
[22] P. Zeppenfeld, M. Kryzowski, C. Romainczyk, G. Comsa, and M. G. Lagally, Phys. Rev. Lett. **72**, 2737 (1994).
[23] J. Tersoff, C. Teichert, and M. G. Lagally, Phys. Rev. Lett. **76**, 1675 (1996).